JMEPEG (1996) 5:637-645

Characterization of the Orientation Structure and Distribution in Rolled Polypropylene

W.B. Lee, S.Z. Wu, and M.S. Song

The polymer orientation structure in rolled polypropylene sheets was studied by polarized-light microscopy, scanning electron microscopy, and wide-angle x-ray diffraction. The initial spherulites became deformed to a pancake shape as rolling deformation proceeded and became more perfectly aligned as the rolling procedure continued. Most polymer crystallites were oriented with their *b*-axis nearly perpendicular to the rolling direction, as shown by x-ray pole figures. Even-order $\langle P_n(\cos\chi)\rangle_c$ coefficients of the Legendre polynomial series ($n = 2$ to 10) describing the *c*-axis or orientation distribution of the molecular chains were determined from measurements of polar angle scan using the transmission technique. The $\langle P_n\rangle_c$ ($n = 2$ to 10) curves calculated from the pseudoaffine deformation theory agreed with the experimental data.

Keywords

orientation distribution, orientation structure, polypropylene

1. Introduction

ORIENTATION structure is an important factor in producing polymer materials with outstanding physical properties. The solid-state deformation of thermoplastics by rolling, extrusion, or drawing remarkably improves mechanical properties such as high modulus, high strength, and good formability in the elongation direction. This enhancement of macroscopic properties stems from the polymer chain orientation that develops during processing. Therefore, characterization of the orientation structure distribution at the molecular level is important in terms of prediction of the properties of oriented materials and better comprehension of the influence of the different processing parameters.

Polarized-light microscopy and scanning electron microscopy (SEM) are the qualitative methods used to observe microstructure as it changes from an original isotropic state to an anisotropic state of lamina at moderate deformation and to a fibrillar state at large deformation. Wide-angle x-ray diffraction (WAXD) is now commonly used in the quantitative study of the molecular orientation in semicrystalline polymers. It provides a direct sampling of the orientation distribution $N(\chi,\psi)$ of the crystal axes with respect to the specimen macroscopic reference directions. This is because the intensity, at a given angle to the meridian, is related to the number of crystallites inclined at some angles to the orientation direction. According to the statistical averages of the orientation distribution function (ODF), this result can be used to quantify the orientation distribution of the crystallites in a polymer. A WAXD investigation of a given crystallographic reflection through the rotation of the χ and ψ angles at a fixed Bragg angle (2θ) gives a pole figure, which is a map of the density of the normal to the investigated crystal plane in the specimen reference system. If the specimen exhibits cylindrical symmetry about its deformation direction (DD), instead of a whole pole figure analysis, the rotation of the specimen around its polar angle χ is sufficient to reveal the orientation distribution $N(\chi,\psi)$ of the crystal axis.

Graphical representations such as polar scans or pole figures yield explicit information on the orientation distribution of a particular crystal plane. However, it is necessary to relate data from different crystallographic reflections to completely describe the molecular orientation that determines the mechanical performance of polymer materials. In addition, reflections from crystal planes that are perpendicular to the polymer chain (*001*) are usually absent or too weak to be analyzed with sufficient accuracy. Thus, the polymer chain orientation distribution must be calculated from measurements made on other crystal planes. Roe and Krigbaum (Ref 1-3) have described the method of pole figure inversion to calculate the orientation of any crystal plane from the measured distribution functions of different (*hkl*) reflections. Their analysis can be applied to an oriented semicrystallite polymer such as polyethylene (PE) or polypropylene (PP) at low or moderate deformation ratio. The crystal orientation is characterized by determining the $\langle P_n\rangle_c$ coefficient of the Legendre polynomial series distribution functions (i.e., Herman's orientation function). In this study, the molecular orientation structure of isotactic polypropylene (i-PP) sheets deformed by rolling to a thickness reduction of 80% was investigated by polarized-light microscopy, SEM, and WAXD.

2. Experimental Method

2.1 *Materials*

Square sheets of i-PP (Goodfellow Cambridge Ltd.), 2.5 mm thick and 100 mm wide with a melt index of 8, were prepared by molding at 200 °C and quenching in water. Transparent oriented sheets were obtained by single-pass rolling at room temperature. The oriented sheets had reduction ratios from 25 to 80%, with thickness ranging from 0.7 to 1.8 mm.

W.B. Lee and **S.Z. Wu,** Department of Manufacturing Engineering, Hong Kong Polytechnic, Hung Hom, Kowloon, Hong Kong; and **M.S. Song,** Department of Polymer Science and Engineering, Beijing University of Chemical Technology, Beijing, China.

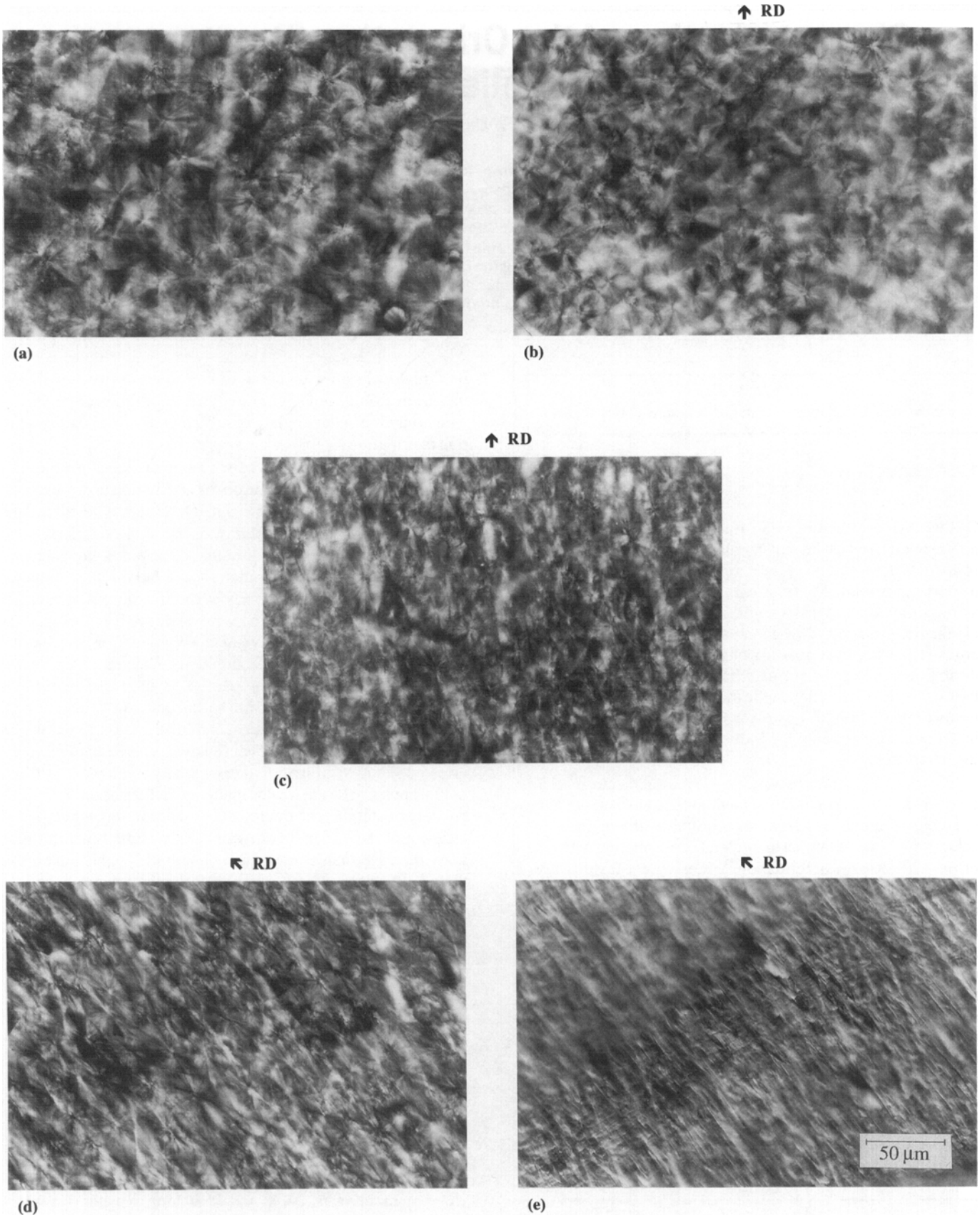

Fig. 1 Optical micrographs, taken through crossed polarizers, of rolled PP sheet for different reduction ratios. (a) 0%. (b) 19%. (c) 33%. (d) 49%. (e) 63%

2.2 *Polarized-Light Microscopy*

Specimens about 18 μm thick were microtomed from the molded PP and rolled PP sheets and observed with a Nikon optical microscope equipped with crossed polarizers. The original sheet was isotropic with spherulites (~45 μm diam), many of which showed a uniform Maltese cross structure. Figure 1 presents five polarized optical microphotographs of i-PP. As deformation proceeds, the spherulite assumes a pancake shape. Figure 2 shows the spherulite deformation schematically. At high reduction ratio, the layer structure is composed of a stacking of deformed spherulite planes. The compression ratio, λ, is defined by d_0/d, where d_0 and d are the sample thickness before and after rolling, respectively, and equals $1/(1 - r)$, where r is the thickness reduction ratio. If the deformation is affine, there is a relationship of $\lambda = D_0/D$ $(= d_0/d)$, where D_0 and D are the diameters of the unrolled and rolled spherulites perpendicular to the rolling direction, respectively. Figure 3 shows D values as a function of the reduction ratio, r. The relation between D and r is almost linear, implying virtually affine deformation. Therefore, the layer order and thickness can be controlled by varying the amount of the reduction ratio and the quenching temperature.

2.3 *Scanning Electron Microscopy*

Samples with different reduction ratios were immersed in liquid nitrogen and broken along the rolling direction to expose their fracture surfaces, which were observed using SEM. The results are shown in Fig. 4. No structural anisotropy was apparent in the original PP sheet, which exhibited flakelike features. These features persisted at a reduction ratio of 75%, although they were definitely elongated in the rolling direction. The appearance of a fibrous texture began at a reduction ratio of about 75%, and the fibrils themselves could be seen at a reduction ratio of 80%. Fracture of the PP by roll drawing produces a similar surface (Ref 4).

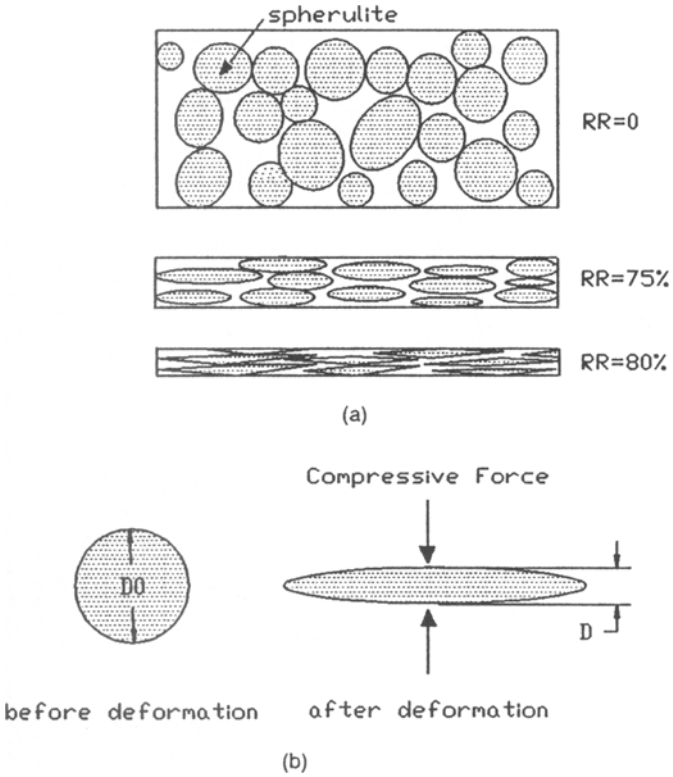

Fig. 2 Schematic of the rolled spherulites in macroscale (a) and on the spherulite scale (b). D_0, diameter of unrolled spherulite; D, diameter of deformed spherulite along the compression direction

2.4 *Wide-Angle X-Ray Diffraction*

Specimens of PP sheets were examined in a Philips x-ray diffractometer (model PW1830) by using nickel-filtered Cu-Kα radiation (0.15406 nm) operated at 40 kV and 35 mA. The incident beam was collimated using a Soller slit with a 1.5 mm pinhole. Detection of the diffracted intensity was provided by a scintillation counter. The geometry of the experimental setup is shown in Fig. 5. All curves for Bragg scan (2θ) and polar scan (χ) were recorded using the transmission technique. For the orientation measurements the polar angle (χ) defining the rotation of the sample around the normal to its surface was rotated from 0° to 90° in half-degree steps, with $\chi = 0°$ corresponding to the rolling direction. The pole figures of (110) and (040) in Fig. 6 were plotted based on the reflection technique, with $\psi = 0°$ corresponding to the rolling direction.

3. Results and Discussion

3.1 *Structural Properties*

The structure of the as-molded and as-rolled isotactic PP can be qualitatively discussed in light of the experimental results. According to the polarized-light and SEM photographs, the original PP sheet exhibited an isotropic structure composed of small spherulites. During rolling, the structure transformed from isotropic to lamellar at moderate deformation and to fibrillar at large deformation. Based on the tie molecule model of

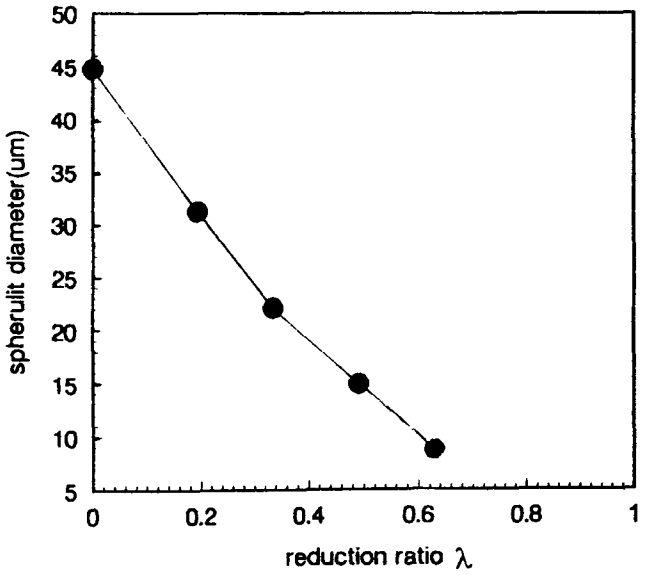

Fig. 3 Relation between spherulite diameter and reduction ratio

Peterlin (Ref 5), the spherulitic structure in the small reduction ratio consists of densely packed parallel lamellae interconnected by a few tie molecules. Deformation at reduction ratios of less than 75% is insufficient to induce the transformation of lamellae to fibrils, since no fibrils were evident in the SEM micrographs shown in Fig. 4(a) to (c). In our study, fibrils were visible at a 75% level of reduction (Fig. 4d). It can be expected that as the reduction ratio increases, modulus and strength could rise as the aspect ratio of the fibrils increases, which could result in better alignment of the molecular chain in the rolling direction. This can also be confirmed by pole figures. Figures 6(a) and (b) are the pole figures of the (110) and (040) crystal planes, respectively, for the rolled PP sheet. Most of the polymer crystallites were oriented with their *b*-axis nearly perpendicular to the rolling direction, and the polymer chains (*c*-axis) were oriented along the rolling direction.

Plots of diffracted intensity against the Bragg angle 2θ had the usual appearance: a sequence of discrete peaks rising from a low, slightly curved baseline. The particular kinds of crystals present determine at which angles of 2θ there will be peaks, and structural features such as the fraction of crystallinity and texture of the specimen influence the actual height or intensity of the peaks. Here, PP crystals of the monoclinic α form with unit cell parameters of $a = 0.667$ nm, $b = 2.084$ nm, $c = 0.6495$ nm, and $\beta = 99.33°$ are expected. Their presence is confirmed by observation of peaks at 2θ equal to 14.10°, 17.00°, 18.56°, 21.27°, and 25.63°, which is in a good agreement with calculated values of 14.12°, 17.01°, 18.55°, 21.35°, and 25.65° for diffraction planes of α-form i-PP corresponding to respective Miller indices of (110), (040), (130), (111), and (060). Table 1 lists the 2θ and φ angles for the different crystal planes that were investigated.

For all samples, the measurements indicate that the orientation distributions of the different crystal reflections are centered at the φ angle defining their inclination with respect to the *c*-axis. Figure 7 presents Bragg angle 2θ scans taken at polar angles (χ) of 0°, 20°, 50°, and 90° for the oriented PP sheet with a reduction ratio of 75%. The molecular chains are aligned in the rolling direction, as can be anticipated in the rolling process.

3.2 *Orientation Distribution Calculations and* $\langle P_n \rangle_c$ *Coefficients*

It is convenient to imagine that the partially oriented polymer can be regarded as an aggregate of units of structure. Determination of its orientation distribution, $N(\chi, \phi)$, which can be achieved by x-ray pole figure measurements, is required in order to characterize the molecular orientation in a polymer sample. For uniaxially oriented polymer samples, the orientation distribution of a given structural unit often exhibits cylindrical symmetry about its deformation direction. The orientation distribution is then reduced to $N(\chi)$, which can be represented by a series in even terms of the Legendre polynomials, $P_n(\cos \chi)$ (Ref 2, 6, 7)

$$N(\chi) = \sum_{n=0}^{\tau} \left(n + \frac{1}{2}\right) \langle P_n(\cos \chi) \rangle P_n(\cos \chi) \qquad \text{(Eq 1)}$$

Table 1 Calculated and experimental values of the Bragg angle (2θ) and the angle φ included between the normal to the (*hkl*) plane and the *c*-axis for different i-PP crystal reflections

	Calculated		Experimental	
(*hkl*)	2θ	φ	2θ	φ
(110)	14.10	90.0	14.12	90.0
(040)	17.00	90.0	17.01	90.0
(130)	18.56	90.0	18.55	90.0
(111)	21.27	50.02	...	...
($\bar{1}$31)	21.84	51.23	21.35	50.19
(041)	21.97	51.51	...	...
(060)	25.63	90.0	25.65	90.0
(022)	29.31	19.41	29.19	19.73
($\bar{1}$12)	29.24	20.01	...	...
($\bar{1}$13)	42.50	11.02	42.53	11.18

where the $\langle P_n(\cos \chi) \rangle$ coefficients are obtained by taking an average over all the orientations in the sample. Only the even $\langle P_n(\cos \chi) \rangle$ values are essential to characterize the crystal plane orientation, since the odd coefficients are equal to zero because of symmetry (Ref 6). For unoriented samples, all coefficients are equal to zero, except the zeroth-order one, which is equal to unity. For a perfect orientation of the structural units along the deformation direction, all the coefficients would be equal to unity.

Calculation of the $\langle P_n \rangle$ coefficient can be made using the equations in Ref 1 and 2:

$$\langle P_n \rangle \equiv \langle P_n(\cos \chi) \rangle = \frac{\int_0^{90} I^*(\chi) P_n(\cos \chi) \sin \chi \, d\chi}{\int_0^{90} I^*(\chi) \sin \chi \, d\chi} \qquad \text{(Eq 2)}$$

where the corrected intensity at an angle χ, $I^*(\chi)$, is achieved by subtracting the background from the minimum value of the intensity in polar scan. The value of the Legendre polynomial of order *n* at the angle χ, $P_n(\cos \chi)$, was computed from the recurrence relation (Ref 2):

$$(n+1)P_{n+1}(\cos \chi) = (2n+1) \cos \chi P_n(\cos \chi) - nP_{n-1}(\cos \chi) \qquad \text{(Eq 3)}$$

Using $P_0(\cos \chi) = 1$ and $P_1(\cos \chi) = \cos \chi$ as starting values, the following coefficients are derived:

$$P_2(\cos \chi) = \frac{1}{2}(3\cos^2 \chi - 1) \qquad \text{(Eq 4a)}$$

$$P_4(\cos \chi) = \frac{1}{8}(35 \cos^4 \chi - 30 \cos^2 \chi + 3) \qquad \text{(Eq 4b)}$$

$$P_6(\cos \chi) = \frac{1}{16}(231 \cos^6 \chi - 315 \cos^4 \chi + 105 \cos^2 \chi - 5) \qquad \text{(Eq 4c)}$$

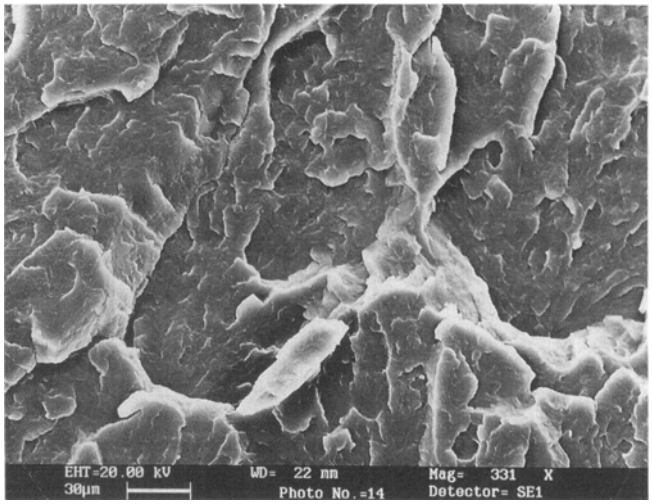

(a)

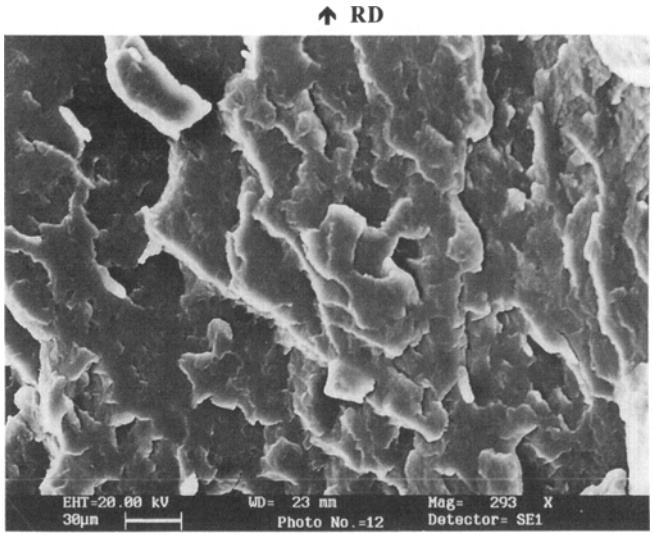

(b)

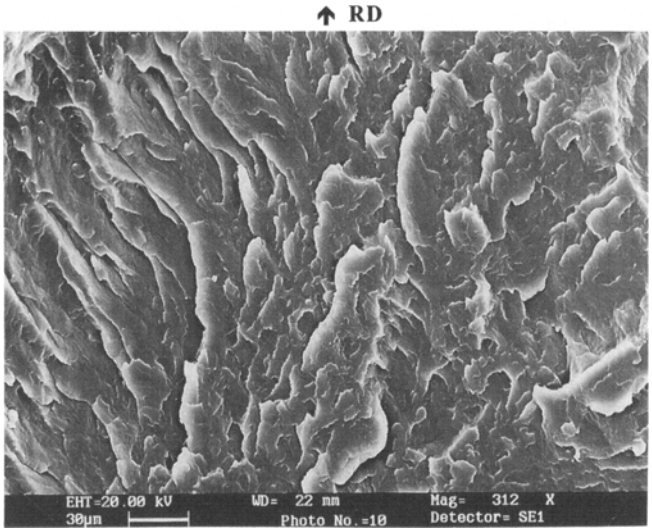

(c)

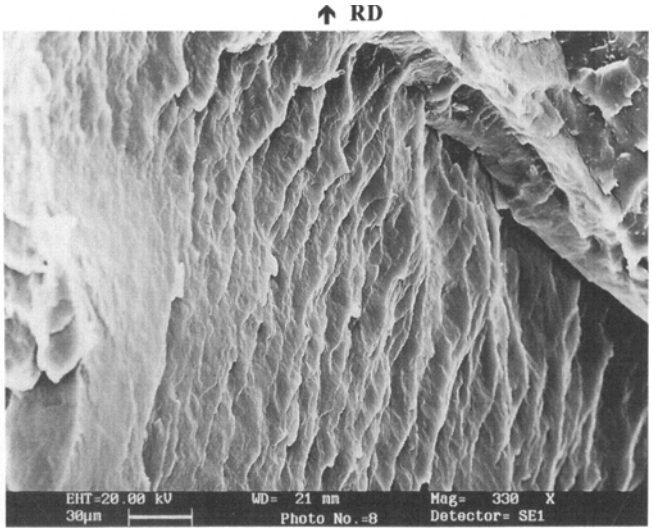

(d)

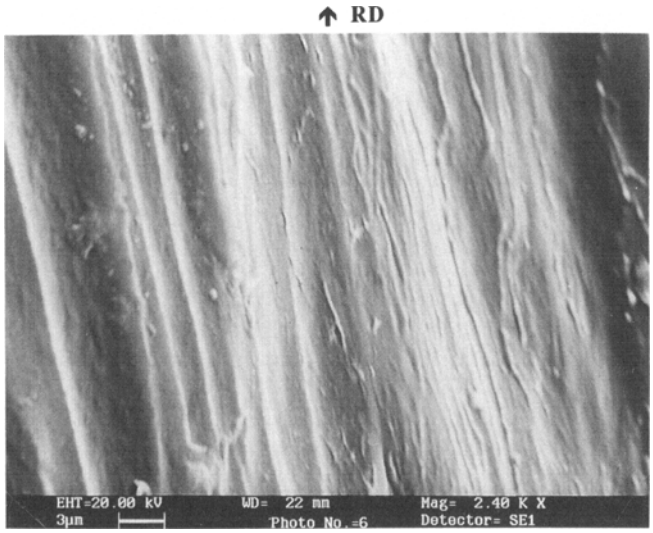

(e)

Fig. 4 SEM micrographs of rolled PP sheets for different reduction ratios. (a) 0%. (b) 50%. (c) 66%. (d) 75%. (e) 80%

$$P_8(\cos\chi) = \frac{1}{128}(6435\cos^8\chi - 12{,}012\cos^6\chi + 6930\cos^4\chi - 1260\cos^2\chi + 35) \quad \text{(Eq 4d)}$$

$$P_{10}(\cos\chi) = \frac{1}{256}(46{,}189\cos^{10}\chi - 109{,}395\cos^8\chi - 30{,}030\cos^6\chi + 3465\cos^4\chi - 63) \quad \text{(Eq 4e)}$$

The numerical integration of Eq 2 was performed using Simpson's rule.

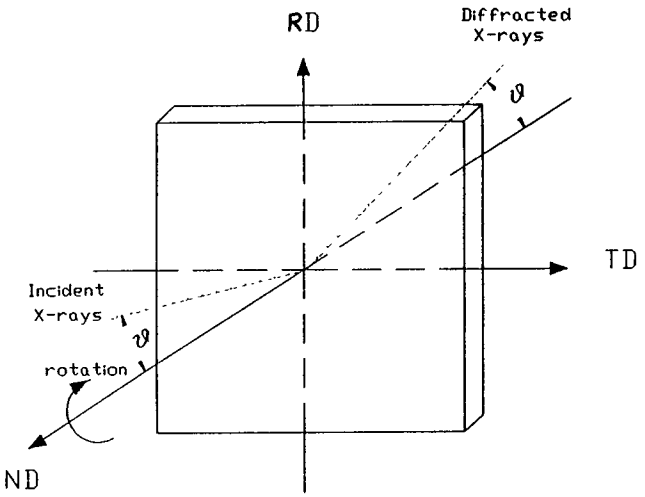

Fig. 5 Experimental setup for orientation measurements by WAXD using symmetrical transmission geometry. RD, rolling direction; TD, transverse direction; ND, normal direction

It is general practice in polymer crystallography to set the *c*-axis parallel to the direction of the molecular chains. For polymers with crystal reflections parallel to the *c*-axis, the coefficients $\langle P_n\rangle_c$ describing the molecular orientation can be acquired directly from x-ray measurements, such as has been done for the (002) crystal planes of oriented PE (Ref 8-10). However, this is not possible for i-PP, which has a monoclinic unit cell and a *(00l)* crystal that is absent in Bragg angle scan. For orientation distributions that have cylindrical symmetry, the Legendre polynomial coefficients relative to the *c*-axis (molecular chain) orientation, $\langle P_n\rangle_c$, can be calculated from the coefficients computed from a given *(hkl)* reflection, $\langle P_n\rangle_{hkl}$ (Ref 8, 10):

$$\langle P_n\rangle_c = \frac{\langle P_n\rangle_{hkl}}{P_n(\cos\phi_{hkl})} \quad \text{(Eq 5)}$$

where ϕ_{hkl} is the angle between the *(hkl)* plane normal and the *c*-axis.

Table 2 $\langle P_n\rangle_c$ coefficients calculated from the experimental orientation distribution for PP sheet with a reduction ratio of 75%

n	(110)	(040)	(130)	(hkl_{av})
2	0.7889	0.7426	0.6680	0.6403
4	0.6860	0.5656	0.4617	0.5732
6	0.4753	0.4842	0.4696	0.3564
8	0.4035	0.3942	0.4243	0.2926
10	0.3128	0.3056	0.3161	0.2119

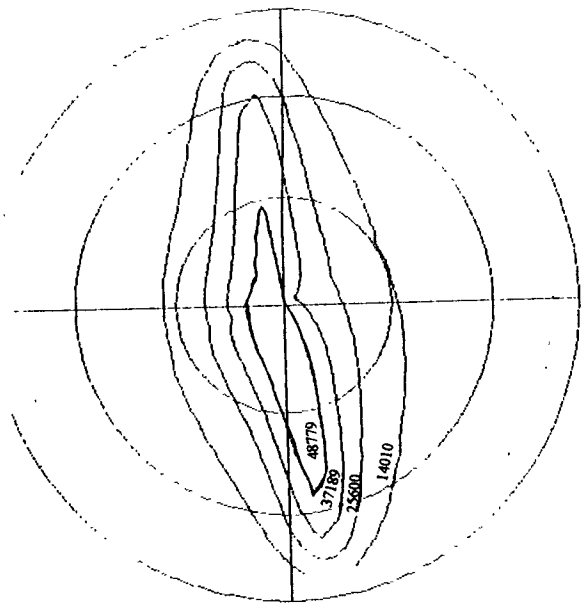

(040)

(a)

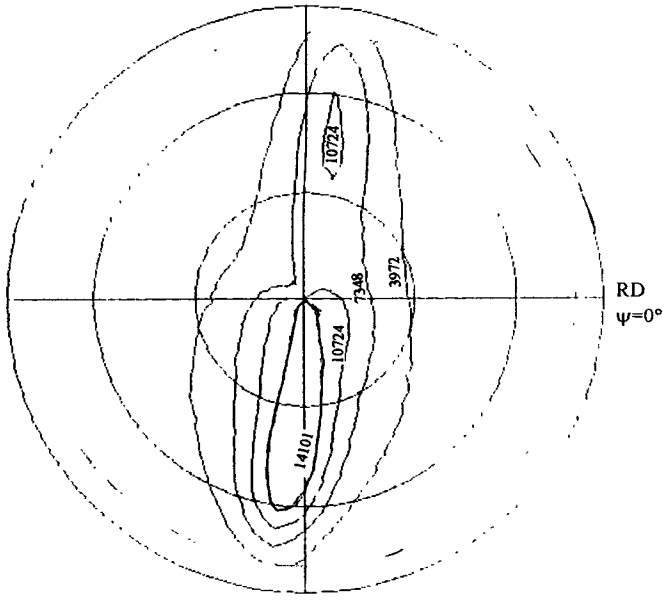

(110)

(b)

Fig. 6 (040) (a) and (110) (b) pole figures of oriented PP with a reduction ratio of 75%

The reflection from (110), (040), (130), and (111)/($\bar{1}$31)/(041) crystal planes are used to calculate the orientation function $\langle P_n \rangle_{hkl}$. Table 2 gives the coefficient $\langle P_n \rangle_c$ values of PP sheet with a reduction ratio of 75%. Figure 8 shows the polar scan results for the different crystal planes studied. The value of the background intensity for each reflection (caused by amorphous and air scattering) was taken equal to the minimum intensity in the baseline region of the scan after smoothing (Ref 11). Because of the weak intensity of (022)/($\bar{1}$12) and ($\bar{1}$13) crystal planes at a low reduction ratio, $\langle P_n \rangle_c$ for the (110), (040), and (130) reflection and the (hkl_{av}) value obtained from the average of (111)/($\bar{1}$31)/(041), (022)/($\bar{1}$12), and ($\bar{1}$13) were calculated (Table 2). Figure 9 shows average $\langle P_n \rangle_c$ values versus λ for n values from 2 to 10. The $\langle P_n \rangle_c$ coefficients are found to increase with λ.

That the deformation of crystalline polymers did not follow the affine deformation scheme of rubber elasticity was an early recognized fact. Crawford and Kolsky (Ref 11) concluded that

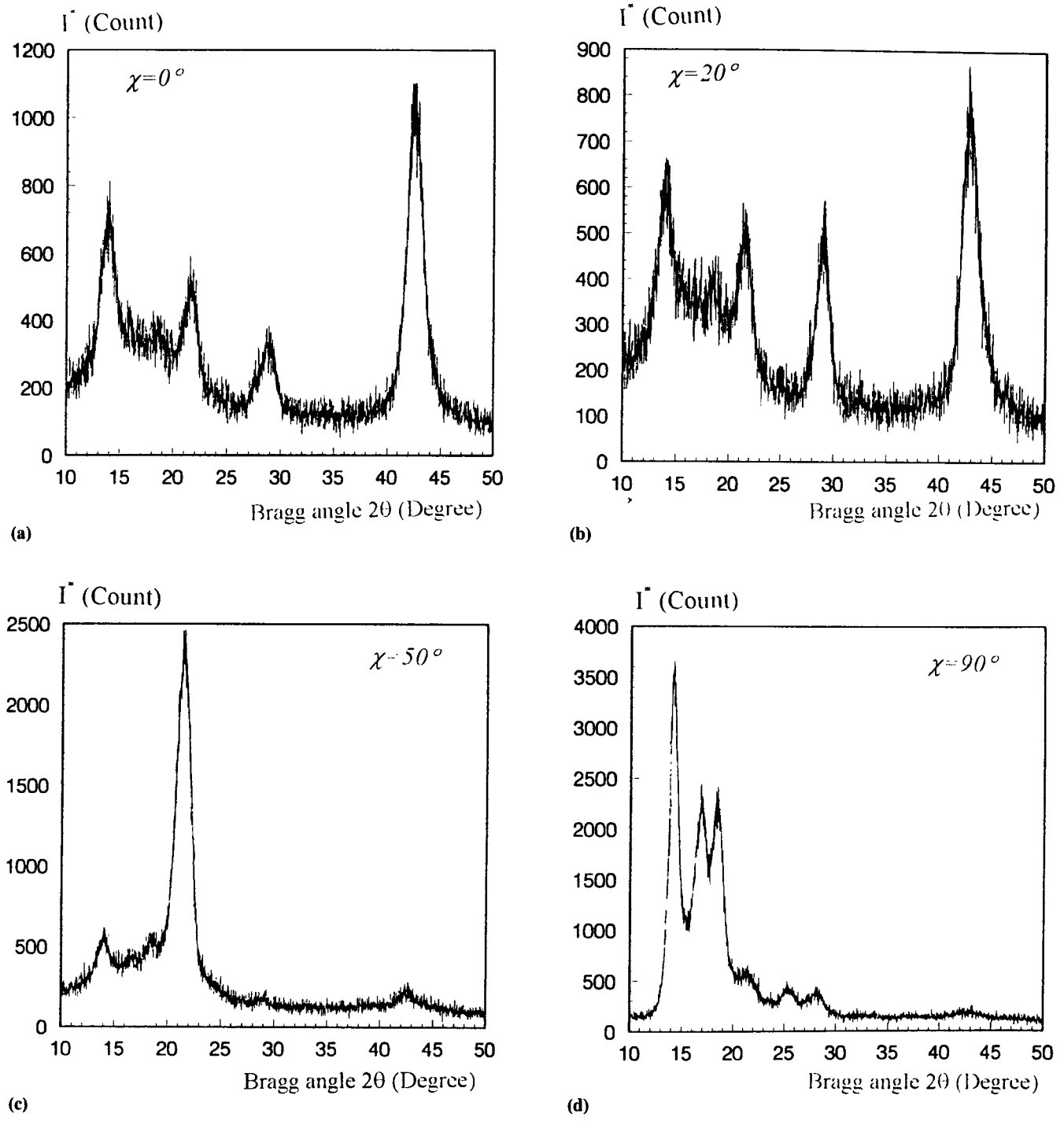

Fig. 7 Bragg angle scans measured for rolled PP with a reduction ratio of 75% at the specified polar angles χ. (a) 0°. (b) 20°. (c) 50°. (d) 90°

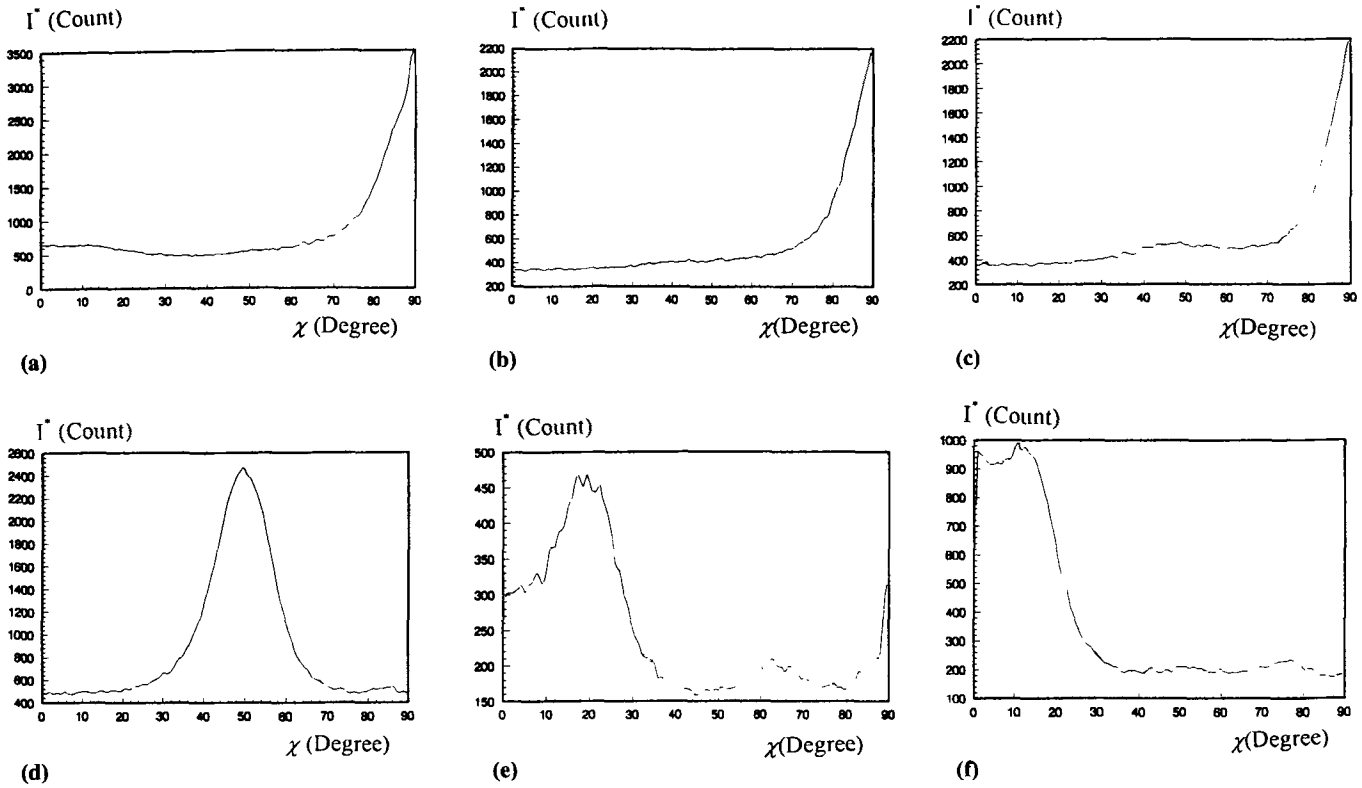

Fig. 8 Polar angle scans measured for rolled PP sheet with a reduction ratio of 75% for six different crystal planes. (a) 110. (b) 040. (c) 130. (d) 111/$\bar{1}$31/041. (e) 022/$\bar{1}$12. (f))$\bar{1}$13

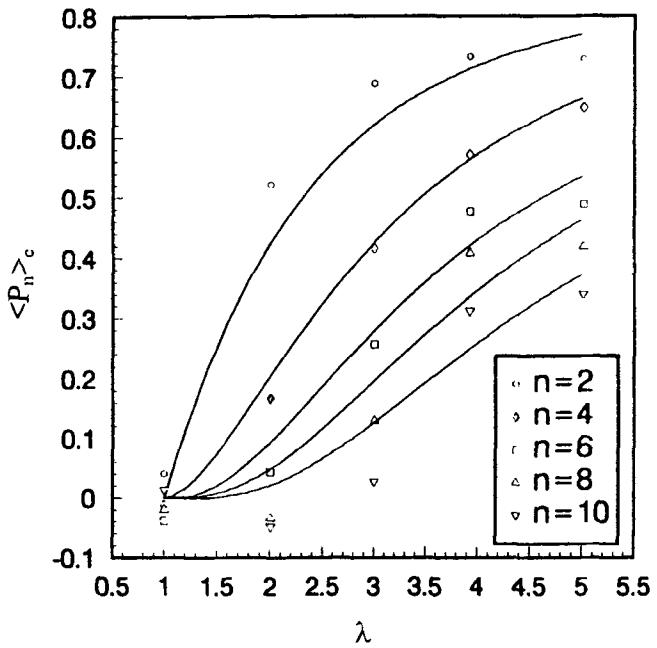

Fig. 9 $\langle P_n \rangle_c$ (n = 2 to 10) theoretical curves compared with experimental data (points)

the birefringence was directly related to the permanent strain, and they suggested a model of rodlike units rotating toward the deformation direction. This deformation model assumes that the polymer is a two-phase system composed of transversely

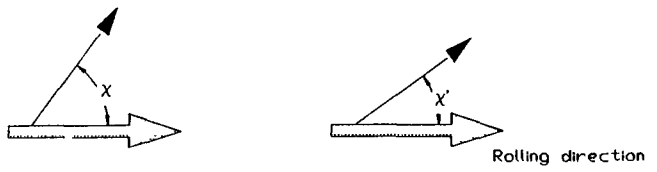

Fig. 10 Pseudoaffine deformation

isotropic rigid units embedded in a deformable matrix. The evolution of orientation proceeds through the rotation of the unique axis of these rigid "floating rods" toward the elongation direction. The fundamental mathematical step in the theory is illustrated in Fig. 10. The orientation of a single unit is therefore defined by the angle between its symmetry axis and the deformation direction. It is supposed that the symmetry axes of the anisotropic units rotate in the same manner as lines joining pairs of points in the macroscopic body, which deforms uniaxially at constant volume. This assumption is similar to the "affine" deformation, but ignores the required change in length of the units on deformation. Such "pseudoaffine" deformation is particularly useful in predicting mechanical anisotropy for crystalline polymers because it enables $\langle P_n \rangle_c$ to be calculated as a function of deformation ratio. The angle χ in Fig. 9 thus changes to χ', and it can be shown that:

$$\tan \chi' = \frac{\tan \chi}{\lambda^{3/2}} \qquad \text{(Eq 6)}$$

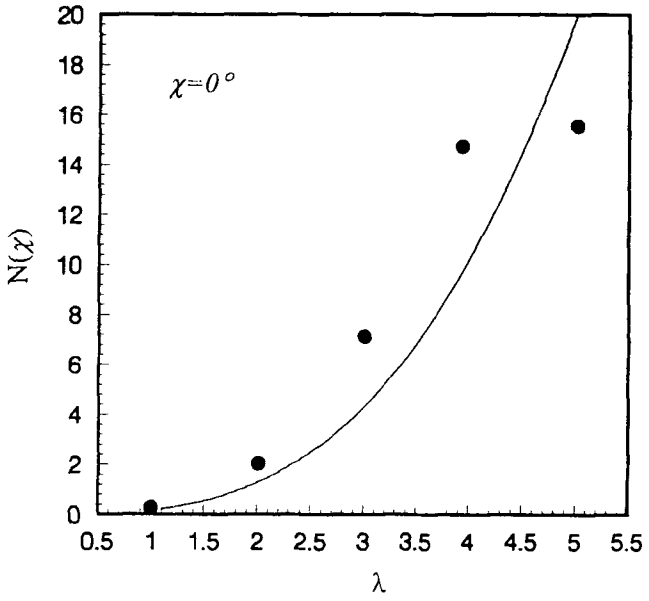

Fig. 11 Theoretical curve of orientation distribution compared with experimental results (points)

where λ is the deformation ratio, equal to the compression ratio λ in rolling procedures. This relationship can be used to calculate the orientation distribution for the units in terms of the compression ratio.

For uniaxial deformation, the resulting orientation distribution of the molecular axis is given by (Ref 12):

$$q(\chi) = \frac{\lambda^3}{2\pi(\cos^2\chi + \lambda^3 \sin^2\chi)^{3/2}} \qquad \text{(Eq 7)}$$

Equation 8 can be used to calculate the coefficients $\langle P_n \rangle_c$ of the *c*-axis (*00l* crystal):

$$\langle P_n \rangle_c = \frac{\int_0^{90} q(\chi) \times P_n(\cos\chi) d\chi}{\int_0^{90} q(\chi) d\chi} \qquad \text{(Eq 8)}$$

The theoretical curves of $\langle P_n \rangle_c$ for *n* values from 2 to 10 versus compression ratio are illustrated in Fig. 9, which shows good agreement with the experimental results calculated from Eq 5. When *n* is equal to 2 or 4, the results are identical with the early conclusions reached by Ward (Ref 13).

Figure 11 is the theoretical curve of the orientation distribution $q(\chi)$ compared with the experimental data $N(\chi)$. The experimental data at a large reduction ratio are lower than the theoretical data by reason of the small *t* value (only 10) used in Eq 1. Thus, at large deformation a large *t* value should be used to calculate $N(\chi)$.

4. Conclusions

In this work, the structural properties obtained during rolling of PP sheet were studied by polarized-light microscopy and SEM. The diameter of the deformed spherulites (pancake thickness) decreased linearly with reduction ratio. Fracture surface studies showed that the initial isotropic structure is displaced by layers of fibrils at high deformation. The replacement by an oriented layered structure is completed at a reduction ratio of about 75%. The polymer chains are aligned along the rolling direction, and the alignment becomes more perfect as rolling proceeds. The theoretical relationship of $\langle P_n \rangle_c$ versus compression ratio for various crystal planes of the monoclinic unit cell of i-PP has been calculated from pseudoaffine deformation theory. The experimental values of $\langle P_n \rangle_c$ coefficients relative to the molecular chain orientation for *n* values from 2 to 10 were determined from WAXD measurements and were found to fit well with the theoretical curves. The orientation distribution of the molecular chains, which cannot be measured directly because of the absence of crystalline reflection parallel to the carbon backbone such as (*00l*), could be calculated by using a series expansion of the Legendre polynomial distribution function.

References

1. R.J. Roe and W.R. Krigbaum, Description of Crystallite Orientation in Polycrystal Materials Having Fibril Texture, *J. Chem. Phys.*, Vol 40 (No. 9), 1964, p 2608-2615
2. W.R. Krigbaum and R.J. Roe, Crystallite Orientation in Materials Having Fibril Texture, Part II: Study of Strained Sample of Cross-linked Polyethylene, *J. Chem. Phys.*, Vol 41 (No. 3), 1964, p 737-748
3. R.J. Roe, Description of Crystallite in Polycrystalline Materials, Part III: General Solution to Pole Figure Inversion, *J. Appl. Phys.*, Vol 36, 1965, p 2024-2031
4. K.R. Tate, A.R. Perrin, and R.T. Woohams, A Tensile Flow Stress Model for Oriented Polypropylene, *Polym. Eng. Sci.*, Vol 28, 1988, p 740-742
5. A. Peterlin, Mechanical Properties of Fibrous Structure, *Ultra-High Modulus Polymers*, A. Ciferri and I.M. Ward, Ed., Applied Science Publishers, London, 1979, p 279-320
6. I.M. Ward, Ed., *Structure and Properties of Oriented Polymers*, Applied Science Publishers, London, 1975
7. A. Ciferri and I.M. Ward, Ed., *Ultra-High Modulus Polymers*, Applied Science Publishers, London, 1979
8. C.P. Lafrance, M. Pezolet, and R.E. Prud'homme, Study of the Distribution of Molecular Orientation in High Oriented Polyethylene by X-Ray Diffraction, *Macromolecules*, Vol 24, 1991, p 4948-4956
9. C.P. Lafrance, J. Debigare, and R.E. Prud'homme, Study of Crystalline Orientation in Drawn Ultra-High-Molecular Weight Polyethylene Films, *J. Polym. Sci., Polym. Phys.*, Ed., Vol 31, 1993, p 255-264
10. C.R. Desper, J.H. Southern, R.D. Ulrich, and R.S. Porter, Orientation and Structure of Polyethylene Crystallized under the Orientation and Pressure Effects of a Pressure Capillary Viscometer, *J. Appl. Phys.*, Vol 41, 1970, p 4284-4289
11. S.M. Crawford and H. Kolsky, Stress Birefringence in Polyethylene, *Proc. Phys. Soc.*, Vol 64B, 1951, p 119-125
12. A. Windle, *Developments in Oriented Polymers*, I.M. Ward, Ed., Applied Science Publishers, London, 1982, chap 1
13. I.M. Ward, Optical and Mechanical Anisotropy in Crystalline Polymers, *Proc. Phys. Soc.*, Vol 80, 1962, p 1176-1188